AIP | Applied Physics Letters

Scaling growth kinetics of self-induced GaN nanowires

Vladimir G. Dubrovskii, Vincent Consonni, Lutz Geelhaar, Achim Trampert, and Henning Riechert

Citation: Appl. Phys. Lett. **100**, 153101 (2012); doi: 10.1063/1.3701591
View online: http://dx.doi.org/10.1063/1.3701591
View Table of Contents: http://apl.aip.org/resource/1/APPLAB/v100/i15
Published by the American Institute of Physics.

Related Articles

Competitive role of Mn diffusion with growth in Mn catalyzed nanostructures
J. Appl. Phys. 111, 084301 (2012)

Stark shifts and exciton dissociation in CdSe nanoparticle grafted conjugated polymer
Appl. Phys. Lett. 100, 151908 (2012)

Nano-precipitates made of atomic pillars revealed by single atom detection in a Mg-Nd alloy
Appl. Phys. Lett. 100, 141906 (2012)

Magnetization enhancement and cation valences in nonstoichiometric (Mn,Fe)3-δO4 nanoparticles
J. Appl. Phys. 111, 074309 (2012)

Nano conductive particle dispersed percolative thin film ceramics with high permittivity and high tunability
Appl. Phys. Lett. 100, 132909 (2012)

Additional information on Appl. Phys. Lett.

Journal Homepage: http://apl.aip.org/
Journal Information: http://apl.aip.org/about/about_the_journal
Top downloads: http://apl.aip.org/features/most_downloaded
Information for Authors: http://apl.aip.org/authors

ADVERTISEMENT

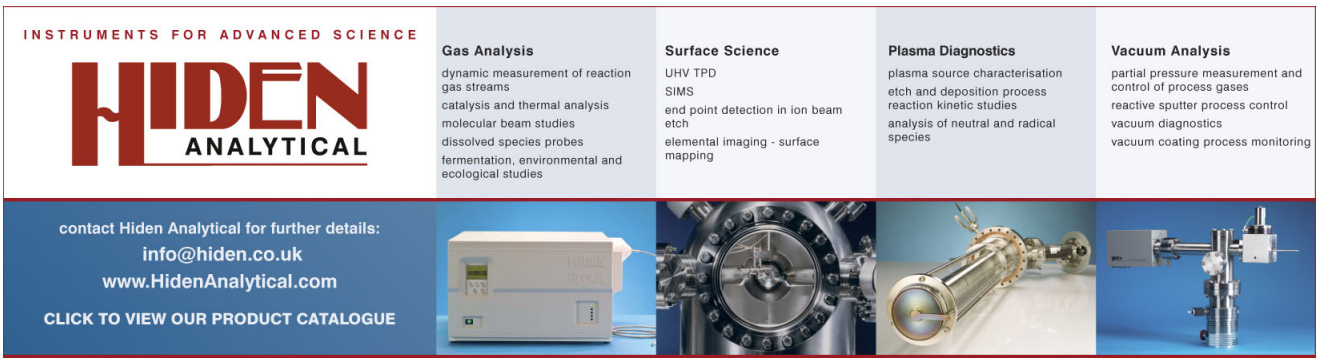

Scaling growth kinetics of self-induced GaN nanowires

Vladimir G. Dubrovskii,[1,2,3,a)] Vincent Consonni,[4,5] Lutz Geelhaar,[4] Achim Trampert,[4] and Henning Riechert[4]
[1]*St. Petersburg Academic University, Khlopina 8/3, 194021 St. Petersburg, Russia*
[2]*Ioffe Physical Technical Institute of the Russian Academy of Sciences, Politekhnicheskaya 26, 194021 St. Petersburg, Russia*
[3]*St. Petersburg State University, Physical Faculty, Peterhof, 198904 St. Petersburg, Russia*
[4]*Paul-Drude-Institut für Festkörperelektronik, Hausvogteiplatz 5-7, 10117 Berlin, Germany*
[5]*Laboratoire des Matériaux et du Génie Physique, CNRS–Grenoble INP, 3 parvis Louis Néel 38016 Grenoble, France*

(Received 16 February 2012; accepted 21 March 2012; published online 9 April 2012)

We present a kinetic model showing why self-induced GaN nanowires synthesized by molecular beam epitaxy obey the scaling growth laws. Our model explains the scaling behavior from kinetic considerations of the step flow radial growth and the shadow effect. The nanowire length L and radius R scale with time as $[1+C(t-t_0)]^{\alpha/(\alpha+1)}$ and $[1+C(t-t_0)]^{1/(\alpha+1)}$, respectively. Consequently, the length scales with the radius as $L \propto R^{\alpha}$. The power index α equals 2.46 in our conditions. This scaling behavior is paramount for understanding the self-induced growth of nanowires in general as well as for tuning their morphology to the desired properties. © *2012 American Institute of Physics*. [http://dx.doi.org/10.1063/1.3701591]

Semiconductor nanowires (NWs) have recently gained much attention from the viewpoints of fundamental properties and possible implication as building blocks of future nanoelectronic,[1] nanophotonic,[2] and nanosensing[3] devices. In particular, self-induced GaN NWs grown on silicon substrates[4–11] enable a dramatic reduction of dislocation density, thus opening a new way for the monolithic integration of optical nanostructures with otherwise unattainable properties with the existing microelectronic platform. However, many important features of the self-induced growth of NWs are not well understood so far. In contrast to NWs obtained by the catalytic vapor-liquid-solid (VLS) process,[1–3,12–15] self-induced GaN NWs start from the Volmer-Weber three-dimensional islands that nucleate on the surface at the growth initial step.[4,7–9,11] In Ref. 16, we have considered the thermodynamic driving force for the island-to-NW shape transformation in the case of GaN NWs grown on Si(111) substrates covered with an amorphous Si_xN_y interlayer. It has been shown that the transformation is driven by the anisotropy of surface energies[9] coupled with the growth anisotropy such that the NW length increases super-linearly with the radius following the scaling dependence $L \propto R^{\alpha}$. The power index α is larger than one and has been found to equal 2.46 in our conditions of molecular beam epitaxy (MBE). However, neither physical explanation nor theoretical consideration is known by this end to support such a scaling behavior.

In this paper, we present more experimental data on GaN NWs synthesized by MBE, demonstrating the scaling length-time, radius-time, and consequently the length-radius dependences. We then develop a theoretical model that is capable of explaining the observed scaling from kinetic considerations. The scaling growth law provides explicitly the time dependences of NW length and radius, showing a good fit with the experimental data. The scaling properties are paramount for understanding the self-induced growth of NWs in general as well as for controling their morphology during MBE growth.

GaN NWs were grown on Si(111) substrates by plasma-assisted MBE as described in Refs. 8, 9,16 and 17. In brief, the active nitrogen species and gallium atoms were supplied by a plasma source and by an effusion cell, respectively. Prior to NW growth, the substrates were exposed to an active nitrogen flux for 5 min, resulting in the formation of a continuous Si_xN_y amorphous interlayer with a thickness of about 2 nm. The nominal gallium and nitrogen rates were fixed to 0.28 and 0.045 nm/s, respectively; the substrate temperature T was kept constant at 780 °C in all experiments, while the growth time was varied. In-situ reflection high energy electron diffraction (RHEED) measurements were performed with an incident electron beam angle to the substrate of 3°. As discussed in Ref. 8, the total growth time for the self-induced approach is the sum of the incubation time necessary for the nucleation of spherical cap islands, of the transition time required for the shape transformation to NWs, and of the actual (i.e., elongation) growth time corresponding to the NW growth phase. In our experiments, the actual NW growth time was varied from 270 to 22 770 s.

The length L and radius R of individual NWs were assessed from transmission electron microscopy (TEM) and field-emission scanning electron microscopy (SEM) images of samples grown for different times. The NW length and radius were assessed among a population of more than 50 NWs, taking into account both the incubation and the transition time that are needed before the NW growth starts and the coalescence effects at a later growth stage. Symbols in Fig. 1 present the measured length-radius dependence, with typical SEM images shown in the inserts. The curve in Fig. 1 corresponds to the power law fit $L = 0.132\,R^{2.46}$ giving the scaling super-linear behavior.[16] The length-time and radius-time dependences will be discussed later on. Despite that the experimental data are noisy due to the random character of

a)Electronic mail: dubrovskii@mail.ioffe.ru.

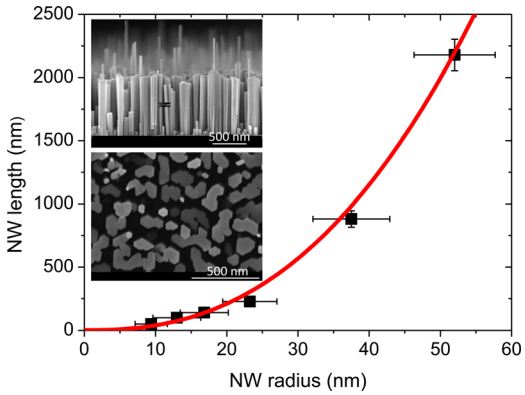

FIG. 1. Scaling length-radius dependence of self-induced GaN NWs: the experimental curve (symbols) fitted by the power law $L = 0.132\ R^{2.46}$; the inserts showing typical plan (a) and top view (b) SEM images of samples grown for 3 h.

NW nucleation (particularly for shorter times), our findings clearly demonstrate that the NWs have a small aspect ratio of the order of one right after the shape transformation but then become highly anisotropic because their length increases with time much faster than the radius.[6,16] This feature should be considered fundamental in the self-induced approach and requires a new theoretical insight into the kinetics of GaN NW growth.

Our model of self-induced, Ga-limited NW growth is illustrated in Figs. 2 and 3. In Fig. 2, we consider a single NW, while Fig. 3 shows the shadow effect on the given NW originating from the neighboring NWs. The cylindrical NW having the length L and radius R at time t elongates due to the direct impingement from the beam intercepting the top facet and the surface diffusion. The diffusion length of Ga adatoms on the NW sidewalls, denoted as λ, is limited by either desorption or incorporation and amounts to only few tens of nanometers at the typical MBE temperatures.[6,10,17] This is the main difference between the growth of GaN and other III-V NWs, where the diffusion length is usually very large, of the order of several micrometers.[13–15,18] As long as L is smaller than λ, all Ga atoms will reach the top and contribute into the NW elongation. Radial extension at $L < \lambda$ is unlikely.

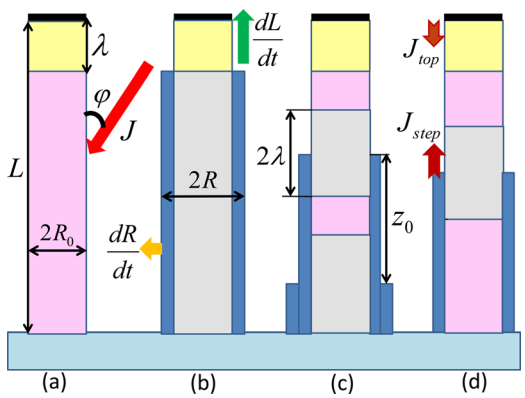

FIG. 2. Schematics of different growth scenarios for a single NW (low NW density): yellow part—NW surface contributing to the elongation, magenta parts—desorption areas, grey parts—radial growth, blue layers show the growing shells; (a)—no radial growth, (b)—radial growth by the sidewall nucleation, (c)—radial growth by the step flow with many steps, (d)—radial growth by the step flow with just one step anytime.

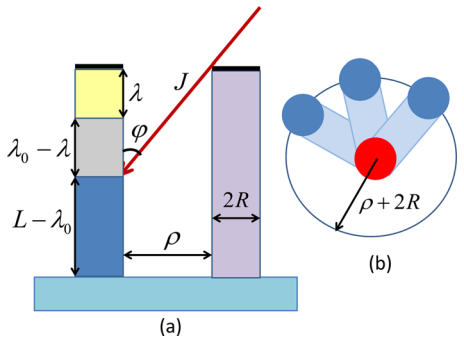

FIG. 3. Shadow effect on a given NW (high NW density): (a)—shadowing decreases the sidewall collection height from $L - \lambda$ to $\lambda_0 - \lambda$, (b)—shadowed zones showing that in a dense NW forest the influx onto the bottom part of the height $L - \lambda_0$ in (a) gets almost completely blocked.

After this short stage (say, after time t_0 from the beginning of deposition), the NW length will exceed the length $L_0 \sim \lambda$, and the growth will acquire the steady state character. Gallium atoms collected by the topmost NW part of height λ migrate to the top facet. The elongation rate of a NW with $L \geq L_0$ is therefore given by the conventional equation[14,17]

$$\frac{\pi R^2}{\Omega}\frac{dL}{dt} = \left(\frac{\chi_f J \sin\varphi}{\pi} - J_{top}\right) 2\pi R\lambda + (\chi_{top} J\cos\varphi - J_{des})\pi R^2. \tag{1}$$

The left hand side describes the net flux of Ga adatoms into the NW contributing to its elongation, with Ω as the elementary volume of a GaN pair in the solid. The first term in the right hand side stands for the resulting diffusion flux collected from the area $2\pi R\lambda$ of the topmost NW part at the arrival rate J making the angle φ to the NW growth axis. The χ_f is the accommodation coefficient at the sidewalls accounting for possible scattering of Ga. The coefficient $1/\pi$ in the arrival rate is the geometrical factor of MBE growth showing that the beam sees the surface area $2R\lambda$, not $2\pi R\lambda$. The parameter J_{top} represents the reverse flux of gallium from the top facet to the sidewalls, which equals the arrival rate at the equilibrium conditions.[13–15,17] All gallium atoms diffusing from the top will evaporate. The second term accounts for the direct impingement onto the top facet ($\chi_{top} J\cos\varphi$, with χ_{top} as the accommodation coefficient at the top) and desorption from the top facet (J_{des}).

Gallium atoms collected by the remaining surface area of NW sidewalls, $2\pi R(L - \lambda) \cong 2\pi RL$ at $L > L_0$, may contribute to the radial growth. Denoting the percentage of Ga adatoms that can reach the incorporation sites as ψ, we can write quite generally

$$\frac{2\pi RL}{\Omega}\frac{dR}{dt} = \left(\frac{\chi_f J \sin\varphi}{\pi} - J_{SW}\right) 2\pi RL\psi. \tag{2}$$

Here, J_{SW} is the desorption flux of gallium from the sidewalls, which equals the arrival rate when no lateral growth occurs. Introducing the equivalent deposition rate, $V = \Omega J\cos\varphi$, Eqs. (1) and (2) can be put in the form

$$\frac{1}{V}\frac{dL}{dt} = \frac{a}{R} + c;\ \frac{1}{V}\frac{dR}{dt} = B\psi, \tag{3}$$

where $a = (2\chi_f g_f \lambda \tan\varphi)/\pi$, $c = \chi_{top} g_{top}$, $B = (\chi_f g_{SW} \tan\varphi)/\pi$, $g_f = 1 - (\pi J_{top})/(\chi_f J \sin\varphi)$, $g_{top} = 1 - J_{des}/(\chi_{top} J \cos\varphi)$, and $g_{SW} = 1 - (\pi J_{SW})/(\chi_f J \sin\varphi)$. The constant growth rate c in the first Eq. (3) can often be neglected, because the sidewall collection is more efficient than that of the top facet for sufficiently small radii. With a time-independent R, this yields the typical diffusion-like length-radius dependence of the form[6] $L \propto 1/R$ at a given moment of time.

We first consider the incorporation probability ψ for a single NW. Four possible scenarios of sidewall incorporation are illustrated in Fig. 2. If the diffusion length is limited by desorption ($\psi = 0$, Fig. 2(a)), all adatoms collected by the lower part of NW would re-evaporate, and the growth would proceed at a constant radius determined at the nucleation stage (where the island to NW growth transformation occurs[9,16]). Growth with a constant radius is not typical for our self-induced GaN NWs, as demonstrated by Fig. 1. Under the conditions shown in Fig. 2(b), all adatoms collected by the sidewalls would be incorporated into the NW, yielding $\psi = 1$. Integrating the second Eq. (3) with the initial condition $R(t = t_0) = R_0$ (where R_0 is the radius acquired at the nucleation stage) readily gives $R(t) = R_0 + BV(t - t_0)$. Inserting this into the first Eq. (3) and integrating, we obtain a combination of linear and logarithmic growth laws, $t - t_0$ and $\ln(t - t_0)$, showing that the length cannot increase super-linearly with R. Since the case of $\psi = 1$ corresponds to the diffusion length limited by the sidewall nucleation,[19] which normally happens at low temperatures, our considerations well explain why self-induced GaN NWs can be obtained only at relatively high growth temperatures.[4–11,16,17]

Scenarios shown in Figs. 2(c) and 2(d) relate to the core-shell radial growth by the step flow. The shells most probably start from the base, since the NW-substrate rectangular interface provides a perfect site to create the step.[10] In this case, the incorporation probability is given by $\psi = (2\lambda)/z_0$, where z_0 is the distance between the steps[20] (Fig. 2(c)). If z_0 is smaller than L, the NW would become tapered, with the inclination angle of the sidewalls to the NW growth axis given by $\tan\beta = h/z_0$ (where h is the height of the step). Tapering is not typical for self-induced GaN NWs. The only possibility to preserve the cylindrical geometry in the step flow model thus yields $z_0 = L$ and $\psi = (2\lambda)/L$, that is, just one surface step on the sidewalls anytime (Fig. 3(d)).

Let us now see how the shadow effect influences the NW growth by MBE. As shown in Fig. 3, the bottom part of given NW is shadowed by the neighboring NWs, so that only the top part of length $\lambda_0 = \rho \cot an\varphi$ (where $\rho \cong 1/\sqrt{\pi N}$ is the average spacing between the NWs and N is the NW density) is exposed to the Ga flux. The lower part is blocked out when the Ga beam is intercepted with one of neighboring NWs (Fig. 3(b)). Under the assumption of a dense NW forest, it can be said that almost no atoms impinge the sidewalls below the height $L - \lambda_0$. If the surface nucleation is enabled everywhere on the sidewall surface exposed to the flux, the incorporation probability in a dense NW array is given by $\psi = (\lambda_0 - \lambda)/L$.

With neglect of c in the first Eq. (3), the kinetic equations in the growth modes presented in Figs. 2(d) and 3 (more generally, whenever ψ is inversely proportional to L) take the form

$$\frac{1}{V}\frac{dL}{dt} = \frac{a}{R};\ \frac{1}{V}\frac{dR}{dt} = \frac{b}{L}. \tag{4}$$

Here, $b = (2\chi_f g_{SW} \lambda \tan\varphi)/\pi$ for the step flow growth and $b = [\chi_f g_{SW}(\lambda_0 - \lambda)\tan\varphi]/\pi$ for the nucleation-mediated growth of a shadowed NW. Integrating this system with the initial conditions $L(t = t_0) = L_0$ and $R(t = t_0) = R_0$ leads to the scaling growth laws of the form

$$L = L_0\left[1 + \frac{(\alpha+1)}{\alpha}\frac{aV(t-t_0)}{L_0 R_0}\right]^{\alpha/(\alpha+1)},$$
$$R = R_0\left[1 + \frac{(\alpha+1)}{\alpha}\frac{aV(t-t_0)}{L_0 R_0}\right]^{1/(\alpha+1)}, \tag{5}$$

$$L = L_0\left(\frac{R}{R_0}\right)^{\alpha}. \tag{6}$$

The power index α is given by

$$\alpha = \frac{a}{b} = \frac{\chi_f J \sin\varphi - \pi J_{top}}{\chi_f J \sin\varphi - \pi J_{step}}, \alpha = \frac{2[\chi_f J \sin\varphi - \pi J_{top}]}{(\lambda_0/\lambda - 1)[\chi_f J \sin\varphi - \pi J_{SW}]}, \tag{7}$$

for the step-flow growth and for the shadowed NWs, respectively. Therefore, the scaling index depends not only on the material parameters but also on the growth conditions. The quantity J_{step} in Eq. (7) equals J_{SW} for the step flow growth. This term originates from the reverse diffusion flux from the step (see Fig. 3(d)).

The general condition for the super-linear growth is given by the inequality $\alpha > 1$. For the step flow, this is reduced to $J_{step} > J_{top}$, the condition which seems reasonable. Indeed, the reverse diffusion fluxes from the top and the step should be proportional to the equilibrium adatom concentrations on the top facet and on the sidewalls, respectively. The NW elongation must proceed by successive nucleation of NW monolayers, which requires sufficient adatom supersaturation on the top facet.[14] This supersaturation is achieved by the gallium deposition from the beam. Same deposition process does not provide high enough supersaturation on the sidewalls to onset the nucleation there, so that the radial growth proceeds by the step flow alone. This strongly suggests that the equilibrium adatom concentration on the sidewalls is noticeably larger than on the top facet, yielding the inequality $J_{step} > J_{top}$ during the entire growth process. As for the shadow effect, typical values of $\lambda_0 = 147$ nm at $N = 10^{10}$ cm^{-2}, $\varphi = 21°$, and $\lambda = 45$ nm (Ref. 17) yield $2/(\lambda_0/\lambda - 1) \cong 1$, so that the inequality $\alpha > 1$ can be easily ensured at $J_{SW} > J_{top}$.

The scaling growth behavior is very important for deducing useful information regarding the kinetic parameters. Indeed, measuring the length-radius, length-time, and radius-time dependences and fitting them by Eqs. (5) and (6) enables the determination of the scaling index α and the effective diffusion length a. As follows from Fig. 1, our

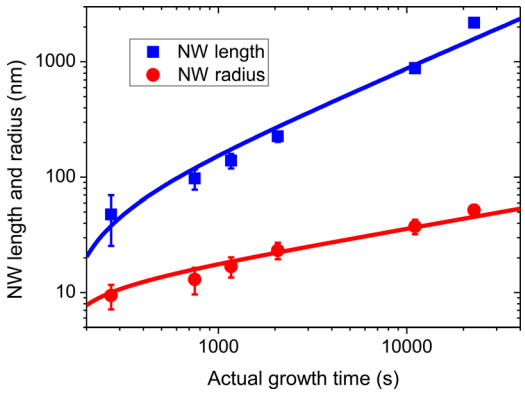

FIG. 4. Experimental length-time and radius-time dependences (symbols) fitted by Eqs. (5) at $\alpha = 2.46$, $a = 51$ nm, $L_0 = 38$ nm, $R_0 = 10$ nm, $t_0 = 270$ s, and $V = 0.045$ nm/s.

self-induced GaN NWs follow the scaling growth law with $\alpha = 2.46$. This yields the values of $\alpha/(\alpha+1) = 0.711$ and $1/(\alpha+1) = 0.289$ for the scaling indices of the time dependences of the NW length and radius, respectively. Symbols in Fig. 4 are the measured $L(t)$ and $R(t)$ dependences. Lines in Fig. 4 correspond to the fits by Eq. (5), obtained at $a = 51$ nm, $L_0 = 38$ nm, $R_0 = 10$ nm, and $t_0 = 270$ s, with $V = 0.045$ nm/s. It is seen that the scaling Eq. (5) describes quite well the time evolutions of the averaged NW length and radius which are indeed sub-linear in the entire time domain. Furthermore, these parameters yield exactly the scaling $L(R)$dependence shown by line in Fig. 1. The discrepancy observed for the longest growth time of 22700 s in Fig. 4 is most probably explained by the influence of direct impingement onto the NW top facet [the omitted c term in Eq. (3)], whose contribution increases for larger R.

In conclusion, we have demonstrated the scaling length-time, radius-time, and consequently length-radius growth laws of self-induced GaN NWs obtained by MBE. Our kinetic model shows that the scaling laws can originate from the core-shell radial growth by the step flow for low NW density (i.e., short growth duration) and from shadow effect for high NW density (i.e., long growth duration). A combination of both mechanisms is expected, and the transition between the two predominant growth modes could be observed by changing the NW density. The latter is determined by the density of Volmer-Weber islands emerging at the initial growth step[9,11] and can be controlled by the surface temperature and deposition flux for example.[21] The scaling growth properties of self-induced GaN NWs should be considered fundamental; however, the scaling indices can be tuned by the deposition conditions. This provides a tool to control the NW morphology during growth.

This work was partially supported by different scientific programs of the Russian Academy of Sciences, few grants of the Russian Foundation for Basic Research, contracts with the Russian Ministry of Education and Science, the FP7 projects SOBONA and FUNPROB as well as by the German BMBF joint research project MONALISA.

[1]M. T. Bjork, B. J. Ohlsson, C. Thelander, A. I. Persson, K. Deppert, L. R. Wallenberg, and L. Samuelson, Appl. Phys. Lett. **81**, 4458 (2002).
[2]S. Gradecak, F. Qian, Y. Li, H. G. Park, and C. M. Lieber, Appl. Phys. Lett. **87**, 173111 (2005).
[3]O. Hayden, G. F. Zheng, P. Agarwal, and C. M. Lieber, Small **3**, 2048 (2007).
[4]M. Yoshizawa, A. Kikuchi, M. Mori, N. Fujita, and K. Kishino, Jpn. J. Appl. Phys. **36**, L459 (1997).
[5]M. A. Sanchez-Garcia, E. Calleja, E. Monroy, F. J. Sanchez, F. Calle, E. Muñoz, and R. Beresford, J. Cryst. Growth **183**, 23 (1998).
[6]R. K. Debnath, R. Meijers, T. Richter, T. Stoica, R. Calarco, and H. Lüth, Appl. Phys. Lett. **90**, 123117 (2007).
[7]T. Stoica, E. Sutter, R. J. Meijers, R. K. Debnath, R. Calarco, H. Luth, and D. Grutzmacher, Small **4**, 751 (2008).
[8]V. Consonni, A. Trampert, L. Geelhaar, and H. Riechert, Appl. Phys. Lett. **99**, 033102 (2011).
[9]V. Consonni, M. Hanke, M. Knelangen, L. Geelhaar, A. Trampert, and H. Riechert, Phys. Rev. B **83**, 035310 (2011).
[10]E. Galopin, L. Largeau, G. Patriarche, L. Travers, F. Glas, and J. C. Harmand, Nanotechnology **22**, 245606 (2011).
[11]V. Consonni, M. Knelangen, L. Geelhaar, A. Trampert, and H. Riechert, Phys. Rev. B **81**, 085310 (2010).
[12]R. S. Wagner and W. C. Ellis, Appl. Phys. Lett. **4**, 89 (1964).
[13]V. G. Dubrovskii, N. V. Sibirev, G. E. Cirlin, A. D. Bouravleuv, Yu. B. Samsonenko, D. L. Dheeraj, H. L. Zhou, C. Sartel, J. C. Harmand, G. Patriarche, and F. Glas, Phys. Rev. B **80**, 205305 (2009).
[14]V. G. Dubrovskii, G. E. Cirlin, and V. M. Ustinov, Semiconductors **43**, 1539 (2009).
[15]J. C. Harmand, F. Glas, and G. Patriarche, Phys. Rev. B **81**, 235436 (2010).
[16]V. G. Dubrovskii, V. Consonni, A. Trampert, L. Geelhaar, and H. Riechert, "Scaling thermodynamic model for the self-induced formation of GaN nanowires," Phys. Rev. B (submitted).
[17]V. Consonni, V. G. Dubrovskii, A. Trampert, L. Geelhaar, and H. Riechert, "Quantitative description for the growth rate of self-induced GaN nanowires," Phys. Rev. B (submitted).
[18]E. Dimakis, J. Lahnemann, U. Jahn, S. Breuer, M. Hilse, L. Geelhaar, and H. Riechert, Cryst. Growth Des. **11**, 4001 (2011).
[19]V. G. Dubrovskii, N. V. Sibirev, G. E. Cirlin, M. Tchernycheva, J. C. Harmand, and V. M. Ustinov, Phys. Rev. E **77**, 031606 (2008).
[20]B. Lewis and J. C. Anderson, *Nucleation and Growth of Thin Films*, (Academic, New York, 1978).
[21]V. G. Dubrovskii, G. E. Cirlin, Yu. G. Musikhin, Yu. B. Samsonenko, A. A. Tonkikh, N. K. Polyakov, V. A. Egorov, A. F. Tsatsul'nikov, N. A. Krizhanovskaya, V. M. Ustinov, and P. Werner, J. Cryst. Growth **267**, 47 (2004).